

1 May 14, 2019

2
3 **Ozone and temperature decadal solar-cycle responses, and their relation to diurnal**
4 **variations in the stratosphere, mesosphere, and lower thermosphere, based on**
5 **measurements from SABER on TIMED.**
6

7 **Frank T. Huang^{1*}, Hans G. Mayr^{2*}**

8 ¹University of Maryland, Baltimore County, MD 21250, USA

9 ²NASA Goddard Space Flight Center, Greenbelt, MD 20771, USA

10 *retired

11
12 **Abstract.** There is evidence that the ozone and temperature responses to the solar cycle of ~11
13 years depend on the local times of measurements. Here we present relevant results based on
14 SABER data over a full diurnal cycle, not available previously. In this area, almost all satellite
15 data used are made at only one or two fixed local times, which can be different among various
16 satellites. Consequently, estimates of responses can be different depending on the specific data
17 set. Also, over years, due to orbital drift, the local times of measurements of some satellites have
18 also drifted. In contrast, SABER makes measurements at various local times, providing the
19 opportunity to estimate diurnal variations over 24 hrs. We can then also estimate responses to the
20 solar cycle over both a diurnal cycle and at the fixed local times of specific satellite data for
21 comparison. Responses derived in this study, based on zonal means of SABER measurements,
22 agree favorably with previous studies based on data from the HALOE instrument, which
23 measured data only at sunrise and sunset, thereby supporting the analysis of both studies. We
24 find that for ozone above ~ 40km, zonal means reflecting specific local times (e.g., 6, 12, 18, 24
25 hrs) lead to different values of responses, and to different responses based on zonal means that
26 are also averages over the 24 hours of local time, as in 3D models. For temperature, effects of
27 diurnal variations on the responses are not negligible even at ~30 km and above. We also have
28 considered the consequences of local-time variations due to orbital drifts of certain operational
29 satellites, and for both ozone and temperature, their effects can be significant above ~30 km.
30 Previous studies based other satellite data do not describe their treatment, if any, of local times.
31 Some studies also analyzed data merged from different sources, with measurements made at
32 different local times. Generally, the results of these studies do not agree so well among
33 themselves. Although responses are a function of diurnal variations, this is not to say that they
34 are the major reason for the differences, as there are likely other data-related issues. The effects
35 due to satellite orbital drift may explain some unexpected variations in the responses, especially
36 above 40 km.

37
38 **1.0 Introduction**

39 The understanding of the response of atmospheric ozone and temperature to the solar cycle of
40 ~11 years is important for both scientific and practical reasons. Global responses in the
41 stratosphere, mesosphere, and lower thermosphere have been investigated over decades based on
42 a variety of satellite data.

43 There is evidence that the magnitude of responses to decadal solar cycles depend on the local
44 times at which the measurements are made. For example, Beig et al.,[2012] in analyzing data
45 from the Halogen Occultation Experiment (HALOE), found that derived responses are different
46 at sunrise (6hrs) and sunset (18hrs).

47 However, with few exceptions, the instruments on satellites measure at only one or two local
48 times, which are fixed for the entire mission.

49 Generally, previous studies do not address in detail the issue of diurnal variations of the
50 responses, and there have been no studies describing the variations of the responses over the 24
51 hrs of local time. In the following, we provide estimates of the diurnal variations of the responses
52 over a 24 hrs, which has not been available previously.

53 As noted in Huang et al. [2016b], previous global responses to the 11-year solar cycle based
54 on measurements have been largely based on data from the NOAA operational satellites (which
55 include the Stratosphere Sounding Unit (SSU), the Microwave Sounding Unit (MSU), and the
56 Solar Backscatter Ultraviolet (SBUV) instruments), from the Stratospheric Aerosol and Gas
57 Experiment (SAGE I, II), on the Explorer and Earth Radiation Budget (ERB) satellites, from the
58 Halogen Occultation Experiment (HALOE) on the Upper Atmosphere Research Satellite
59 (UARS), and from the Sounding of the Atmosphere using Broadband Emission Radiometry
60 (SABER) instrument on the Thermosphere-Ionosphere-Mesosphere-Energetics and Dynamics
61 (TIMED) satellite, among others. The advantage of the operational satellites is that they can
62 provide global measurements covering decades, being replaced as needed. However, issues of
63 instrument offsets, stability, and continuity over many years and decades can be problematic.

64 Except for SABER (and UARS), instruments on these satellites make measurements at only
65 one or two local times, which are fixed for the mission duration. The NOAA operational
66 satellites are sun-synchronous, in which case the measurements are made at two fixed local
67 times, one for the ascending orbital mode, and one for the descending mode. HALOE and SAGE
68 make solar occultation measurements, only at instrument sunrise and sunset. Consequently, used
69 as is, responses based on zonal means of the above measurements reflect long term variations at
70 the fixed local times, and could be a source of differences among the various studies.

71 They could also be a source of differences with 3D models, whose ozone amounts and
72 temperature vary with local time around a latitude circle, and whose zonal means are averages
73 over both longitude and 24 hrs of local time. When comparing results of responses based on
74 zonal means from measurements with models, Austin et al. [2008] point out that “The model
75 results are strictly zonal average values, which is an average over local time, whereas the
76 observations are typically made at fixed local times. Therefore, in the mesosphere, where the
77 diurnal variation of ozone is large, some of the differences between model results and
78 observations may have arisen from a diurnal variation in the actual solar response”. See also
79 Beig et al. [2012].

80 In addition, the orbits of some operational satellites have drifted, so that the local times at
81 which the measurements are made have also drifted over several hours or more (see McPeters et
82 al. [2013], Frith et al. [2014], Remsberg [2008], Randel et al. [2009], Tummon et al. [2015],
83 Hood et al. [2015]). Tumman et al. [2015] summarizes some of the data processing methods
84 taken by various groups. Generally, they report that diurnal variations are either neglected, or are
85 assumed to be negligible below ~ 45 -50 km. See also Davis et al. (2015).

86 Previous results have not generally agreed so well with one another in their details. A major
87 reason for these differences may be the conditions and constraints under which the various
88 measurements were made. For details, see Austin et al., [2008], Crooks and Gray [2005], Gray et
89 al. [2005], Huang et al. [2016b].

90 In addition, previous studies generally have not described how they treat diurnal variations, so
91 that comparisons related to responses as a function of local times are problematical. We are also
92 not aware of studies based on orbital drift.

93 In contrast to most other measurements, SABER provide additional information which allows
94 us to estimate daily ozone and temperature diurnal variations, and then also the dependence of
95 their responses to the decadal solar cycle on local time. In the following, we focus on zonal
96 means of ozone and temperature, either at various specific local times, or averaged over local
97 times (as in 3D model), and the effects of their diurnal variations on their responses to solar
98 variability over a solar cycle of ~ 11 years (2002-2014), from 20 to 100 km.

99 In this study, we find that not only do the values of the responses depend on the local times at
100 which the measurements are made, but they can be significant even at altitudes as low as 30 km.

101 In Section 2, we review our previous analysis and derivation of diurnal variations and zonal
102 means that are averages of both longitude and local time around a latitude circle, based on
103 SABER measurements. We also describe how we can estimate new results of zonal means
104 corresponding to specific local times, and new results in estimating effects of orbital drift on
105 diurnal variations.

106 In Section 3 we describe our new results of responses to the solar cycle at the specific local
107 times of sunrise (6hrs) and sunset (18hrs), and compare with results from HALOE. This gives an
108 indication of the quality and reality of our and HALOE's results.

109 In Section 4 we describe our new results of responses to the solar cycle over a diurnal cycle of
110 24 hrs.

111 In Section 5 we describe our estimates of responses in situations where the local times have
112 'drifted' due to satellite orbital drifts. We also describe some previous studies.

113 In Section 6 we discuss the issue of data length.

114 115 **2.0 SABER data characteristics and analysis.**

116 The SABER/TIMED instrument [Russell et al., 1999] was launched in December 2001 with
117 an orbital inclination of $\sim 74^\circ$. SABER views the Earth's limb to the side of the orbital plane, and
118 vertical profiles, corresponding to the line-of-sight tangent point, are retrieved from
119 measurements of the CO_2 15 and 4.3 μm emissions for kinetic temperature, and from the 9.6 μm
120 channel for ozone. About every 60 days, TIMED is yawed by 180° , so that the SABER
121 measurement footprint of SABER spans latitudes $\sim 83^\circ\text{N}$ to 52°S or $\sim 83^\circ\text{S}$ to 52°N on alternate
122 yaw periods. Over a given day and for a given latitude circle, measurements are made as the
123 satellite travels northward (ascending mode) and again as the satellite travels southward
124 (descending mode). Data at different longitudes are sampled over 1 day as the Earth rotates
125 relative to the orbit plane.

126 SABER scans altitude (~ 10 -105 km for temperature, 15-100 km for ozone) every 58s with an
127 altitude resolution of ~ 2 km, with ~ 96 scans per orbit, and ~ 14 longitudes per day.

128 The orbital characteristics of the satellite are such that, over a given day, a given latitude
129 circle, and a given orbital mode (ascending or descending), the local time at which the data are
130 measured is essentially the same, independent of longitude and time of day. For a given day,
131 latitude, and altitude, we work with data averaged over longitude: one for the ascending orbital
132 mode and one for the descending mode, each corresponding to a different local solar time,
133 resulting in two data points for each day. Each can be biased by the local time variations and is
134 therefore not a true zonal mean. True zonal means are averages made at a specific time over
135 longitude around a latitude circle, with the local solar time varying by 24 h over 360° in
136 longitude. The local times of the SABER measurements decrease by about 12 min from day to
137 day, and it takes ~ 60 days to sample over the 24 hrs of local time.

138

139 **2.1 Previous analysis**

140 The data are provided by the SABER project (version 2.0, level2A). They are interpolated to 4-
141 degree latitude and 2.5 km altitude grids, after which zonal averages are taken for analysis.

142 In contrast to other satellite measurements, those from SABER (Russell et al., 1999) contain
143 information to estimate the diurnal variations of ozone and temperature, and the results are
144 described in Huang et al. [2010a, 2010b].

145 As noted in Huang et al. [2016b], SABER ozone and temperature measurements have been
146 analyzed with success for more than a decade. We have derived variations with periods from one
147 day or less (diurnal variations) up to multiple years (semiannual oscillations (SAO) and quasi-
148 biennial oscillations (QBO)), and one decade or more (trends, responses to solar cycle). See
149 Huang et al. [2008a,b, 2010a,b, 2014, 2016a,b]. Zhang et al. [2006] and Mukhtarov et al. [2009]
150 have derived temperature diurnal tides using SABER data, and Nath and Sridharan [2014] have
151 also derived responses to solar variability using SABER data.

152 For both ozone and temperature, these studies show that, for variations that are deviations from
153 a mean state (e.g., diurnal variations, tides, semiannual and quasi-biennial oscillations, responses
154 to solar variability, trends), SABER measurements are robust and precise. For example, zonal
155 mean tidal temperatures can agree with other measurements to within $\sim 1^\circ\text{K}$ (Huang et al.,
156 2010a), and our zonal mean ozone diurnal variations can agree with other diurnal measurements
157 to less than a few percent (Huang et al., 2010b).

158 These previous results contain

- 159 1) diurnal variations of ozone and temperature for each day of the year, and
- 160 2) zonal means that are averages over both longitude and local time in a consistent manner,
161 which can then be compared directly with 3D models.

162
163 Using these, we can then estimate the goals of this study, which is to

- 164 3) reconstruct the zonal means to reflect specific local times.
- 165 4) calculate responses to solar variability over a solar cycle at specific local times
- 166 5) estimate local time variations of responses as a result of orbital drifts of NOAA satellites,
167 as noted above.

168 We can therefore find the variation of responses to the solar cycle over the 24hrs of local time,
169 including at 6 and 18hrs for comparison with responses based on HALOE data at sunrise and
170 sunset for comparison (see Beig et al. [2012], Fadnavis and Beig [2006]).

171 Compared to the stratosphere, diurnal variations of ozone and temperature themselves are
172 more prominent in the mesosphere and lower thermosphere. Even in the stratosphere, they may
173 not be negligible (Huang et al. 2010a, 2010b). Between ~ 30 and 80 km, ozone diurnal variations
174 are due mainly to photochemistry (Brasseur and Solomon, 2005), while temperature diurnal
175 variations are mainly a result of thermal tides (Chapman and Lindzen, 1970). For diurnal
176 variations, our results for both ozone and temperature (Huang et al. 2010a, 2010b) show that they
177 can be systematic from the lower thermosphere down to 25 km. This is consistent with results by
178 Sakazaki et al. [2015] for ozone, and Oberheide et al.[2000] and Gille et al. [1991] for
179 temperature.

180 As discussed below, for responses due to the solar cycle, our results show that the effects of
181 local time variations can be non-negligible for altitudes even below 40 km, especially for
182 temperature.

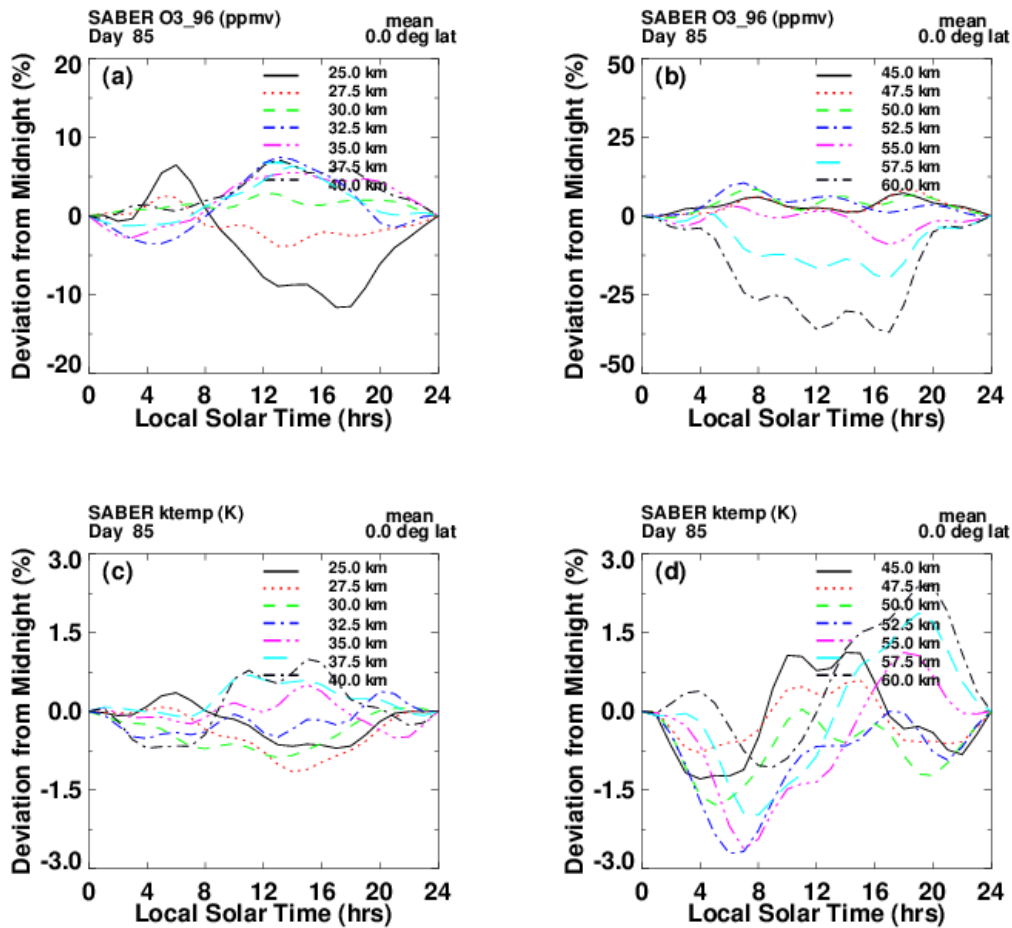
183 184 **2.1.1 Diurnal variations**

185 As noted above, and in Huang et al. [2016b], unlike other satellites mentioned above (except
186 UARS), the orbital characteristics of TIMED are such that SABER samples over the 24 hrs of
187 local time, which can be used to estimate diurnal variations of ozone and temperature. A
188 complication is that it takes SABER 60 days to sample over the 24 hrs of local time. Over 60
189 days, the variations with local time are embedded with the seasonal variations, and need to be
190 separated from them. The method we use estimates both the diurnal and mean variations (e.g.,
191 seasonal, semiannual, annual) together, by performing a least squares fit of a two-dimensional
192 Fourier series, where the independent variables are local time and day of year. The algorithm is
193 discussed further in Huang et al. [2010a,b].

194 The top row of Figure 1 shows zonal mean ozone diurnal variations (percent deviation from
195 midnight) for day 85 of 2005, at the equator, from 25 to 40 km (left panel), 45 to 60 km (right
196 panel), based on SABER data. See Huang et al. [2010b] for details, and references. It can be seen
197 that diurnal variations can be significant even at 25 km. Since the study of Huang et al.,[2010b],
198 Sakazaki et al., have derived comprehensive ozone diurnal variations based on observations from
199 the Superconducting Submillimeter-Wave Limb-Emission Sounder (SMILES) on board the
200 International Space Station (ISS).

201 The bottom row of Figure 1 corresponds to the top row, but for temperature. See Huang et al.
202 [2010a] for details. Even at altitudes near 30 km, the diurnal variations are systematic and, as
203 seen below, can affect results in estimating decadal responses. Although small, at 30 km, the
204 diurnal variations of temperature compare well with Zeng et al. [2008], Oberheide et al.[2000],
205 Gille et al.[1991], based on different types of measurements.

206
207



208
209
210
211
212
213

Figure 1. Top row: ozone zonal mean mixing ratios (ppmv) versus local time for day 05085 at the Equator. Left panel (a): 25 to 40 km (percent deviation from midnight), right panel (b): 45 to 60 km. Bottom row: as in top row, but for temperature (K).

2.1.2 Mean variations.

215 Once the diurnal variations are known for each day, the zonal mean variations, which are averages over longitude and local time, consistent with 3D models, can be obtained.

217 Based on these zonal means, our earlier results of decadal responses to solar activity, as represented by the 10.7 cm solar flux, had been presented in Huang et al. [2016a, 2016b].

2.2 Current analysis

2.2.1 Multiple regression

223 For the current study, as for the previous analysis, we generate diurnal variations and mean variations as well, from which we generate the following:

225 a) monthly zonal means that are averaged over longitude, but at specific local times. These correspond to those satellite measurements which sample at specific local times

227 b) zonal means with local times that vary from month to month, to simulate the situation caused by satellite orbital drifts, as described earlier.

228

229 c) estimates of responses to solar the cycle, based on a) and b), and compare with responses
 230 based on zonal means that are also averaged over local time.

231 As an example, in Figure 2, the left panel (a) shows our ozone monthly mean mixing ratios
 232 (red line, parts per million by volume, ppmv) at 47.5 km and the Equator, from mid 2002 to mid
 233 2014, with seasonal and local time variations removed. The green lines represents how the data
 234 would vary if we simulated the variations with local time due to orbital drifts of the NOAA
 235 operational satellites. We have varied the local times such that from 2002 to 2014, they progress
 236 from 12 to 18 hrs. Also shown is the corresponding 10.7 cm flux (black lines, right axis, units in
 237 sfu). As can be seen, year 2002 was near solar maximum; the middle of solar cycle 23, and 2014
 238 is some years into cycle 24, which began ~2008. The right panel (b) corresponds to the left
 239 panel, but for temperature (K) at 45 km. The labels ‘CRC’ denote the correlation coefficients
 240 between the respective ozone and temperature zonal means and the 10.7 cm flux.

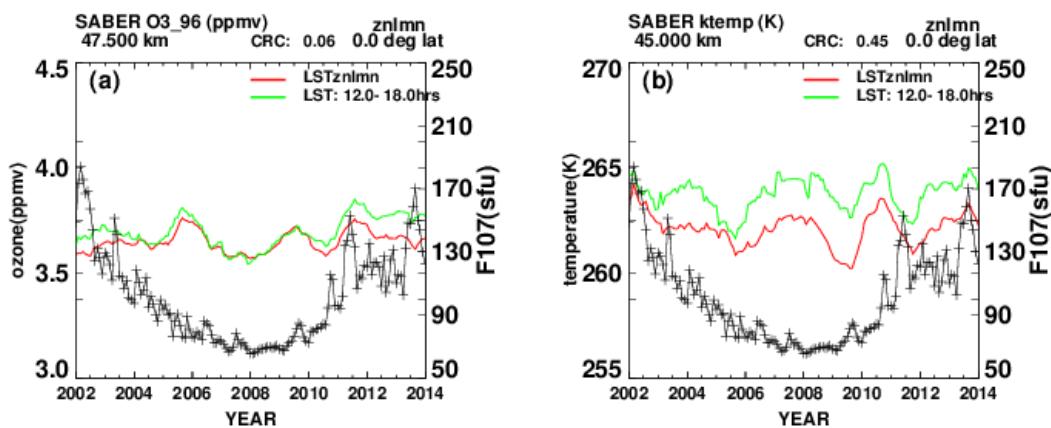
241 The estimates of responses to the solar cycle are made using Equation (1), in a similar manner
 242 as previously done by others, and by us, using a multiple regression analysis (e.g., Keckut et al.
 243 [2005], Soukharev and Hood [2006], Huang et al. [2016b]) that includes solar activity, trends,
 244 seasonal, quasi biennial oscillations (QBO), and local time terms, among others, on monthly
 245 values. Specifically, the estimates are found from the equation

$$247 \quad M(t) = a + b * t + d * F107(t) + c * S(t) + l * lst(t) + g * QBO(t) \quad (1)$$

249 where t is time (months), a is a constant, b is the trend, d the coefficient for solar activity (10.7
 250 cm flux), c is the coefficient for the seasonal (S(t)) variations, l the coefficient for local time (lst)
 251 variations, and g the coefficient for the QBO. As is often done, the seasonal and local time
 252 variations are removed first, but we include them in Equation (1) for completeness. The F107
 253 stands for the solar 10.7 cm flux, which is commonly used as a measure of solar activity, and the
 254 values used here are monthly means provided by NOAA.

255 M(t) stands for the input ozone or temperature zonal means described in a) and b), above.

256 The algorithm is applied to the monthly zonal-mean values from June 2002 through June 2014
 257 (as in Figure 2), from 48°S to 48°N latitude, and from 20 to 100 km.
 258



259 **Figure 2.** Ozone zonal mean mixing ratios (left panel, red line, ppmv) from mid 2002 to mid 2014, 47.5 km, 0° lat;
 260 right panel, as in left panel, but for temperature (K) at 45km. The green lines represent how the data would vary if
 261 we simulated the variations with local time due to simulated orbital drifts of the NOAA operational satellites. Black
 262 lines (+, right scale) show the corresponding monthly 10.7 cm flux (sfu) provided by NOAA.
 263

264

265 **2.2.2 Statistical and error considerations**

266 The analysis of uncertainties is the same for the current study as for the previous study of the
267 mean variations just described. It is only the input data that are different. Previously, the input
268 consisted of zonal means that are averaged over both longitude and local time, as in 3D models.
269 Here the zonal mean reflect measurements made at specific local times. Details of the statistical
270 analysis are given in Huang et al.,[2106a, 2016b].

271 The studies use a least squares fit of the multiple regression of Equation (1). Uncertainties in
272 the responses are found from the sample variance (Bevington and Robinson, 1992, Huang et al.,
273 2016a) of the fit. The curvature matrix and its inversion are quite stable due to the excellent
274 sampling of SABER, as there are essentially no significant data dropouts to speak of. So the
275 standard errors are quite stable and reasonable, as can be seen in the error bars in Figures 6, 7, 8,
276 and A1 and A2, in the Appendix. Although very stable in our case, the inversion of the curvature
277 matrix does not explicitly or definitively address potential aliasing among the various terms of
278 the multiple regression, unless the matrix is diagonal.

279 In Section 6 (Data length and aliasing) below, we show that the derived responses are
280 essentially the same whether we use all the terms in Equation (1) or only the term containing the
281 solar flux to obtain the responses. So aliasing is not an issue here.

282

283 **3.0 Results: Ozone and temperature responses to solar cycle at 6, 18hrs (sunrise and sunset)**

284 Specifically, we use the term ‘response to solar activity (solar cycle)’ generally to refer to the
285 term $d \cdot F_{107}$ in Equation (1), and in particular to ozone or temperature responses at solar
286 maximum minus those at solar minimum, per 100 solar flux units (sfu). For ozone, it is also in
287 terms of percentage differences. A positive response means that the response at solar maximum
288 is larger than that at solar minimum (Huang et al.,2016b).

289 For the new results of this study, we focus on the following:

- 290 1) Responses to the solar cycle at 6 and 18 hrs (sunrise, sunset). Comparisons with
291 responses based on HALOE data (Beig et al. [2012], Fadnavis and Beig [2006]), which measure
292 only at sunrise and sunset.
- 293 2) Responses based on zonal means at specific local times.
- 294 3) Responses with local times changing due to satellite orbital drifts.
- 295 4) Comparison with results based on zonal means that are averages over both longitude and
296 local time simultaneously, as in 3D models.

297

298 **3.1 Ozone responses at 6, 18hrs (sunrise and sunset)**

299 We consider first sunrise and sunset (6, 18hrs) because there are direct empirical results with
300 which to compare, by Beig et al., [2012] and Fadnavis and Beig [2006], based on HALOE data
301 from January 1992 to November 2005. Importantly, unlike other studies, they describe how they
302 treat variations with local times, although they have results only at 6 and 18hrs.

303 The comparisons will indicate the quality of our results at 6 and 18hrs, and also over the 24
304 hrs of local time.

305 In Figure 3 and applicable other figures, we have manually transferred values of plots from
306 other studies for comparison, so they are not exact, but should be adequate for our purposes.

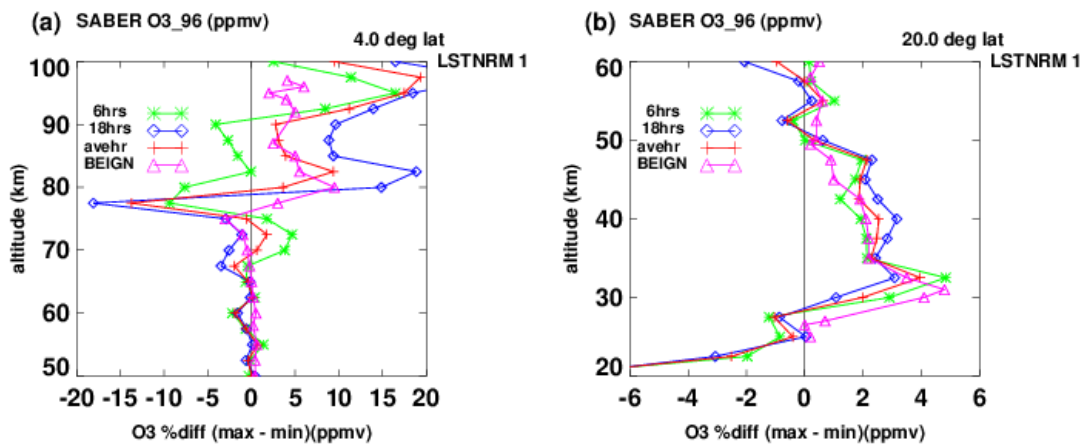
307 In comparisons with results based on HALOE data, uncertainties should be considered.
308 According to Beig et al., [2012] and Fadnavis and Beig [2006], due to the sparse sampling
309 inherent in solar occultation measurements, there are only 8 to 12 data points (sometimes less)

310 per month for each latitude. So they generally present responses that are based on data
 311 composited over 30-degree latitude bins (e.g., 0-30°S, N) and averages of responses at sunrise
 312 and sunset. We get results at 4-degree intervals. Even if we composite the SABER data into 30°
 313 bins, the distribution within the bins would be uniform, but quite different than that of HALOE
 314 data, so we will present our results at specific latitudes. Our responses can vary significantly as a
 315 function of latitude, so that is another consideration in the comparisons.

316 In addition, here and in the literature, ozone responses are normally given in terms of percent
 317 changes, and the value of the ozone itself is needed to get percent values. Because absolute
 318 values among various instruments can sometimes be offset, it is an added source of uncertainty.

319 Figure 3 (left panel) shows our and that of Beig et al.,[2012] ozone responses from 50 to 100
 320 km, at 4°N. The magenta triangles show responses based on HALOE data for ozone (composite,
 321 0-30°N, BEIGN), which are averages of sunrise and sunset responses, and should be compared
 322 with the red plusses, which denote the average of our results at 6hrs and 18hrs. It can be seen that
 323 the agreement of our averages (magenta triangles and red plusses) are very favorable, except for
 324 our large negative value at 77.5 km, and above 90km. The green asterisks denote our results for
 325 6hrs and the blue diamonds denote our responses at 18 hrs. The right panel corresponds to the
 326 left panel, but for 20°N and 20 to 60km, and the HALOE results are from Fadnavis and Beig
 327 [2006], 0-30°N composite. As in the left panel, the agreements of our averages (magenta
 328 triangles and red plusses) are very favorable. It can be seen that even in the stratosphere, the
 329 responses at 6hr are different from those at 18hrs.

330 Considering our discussion of uncertainties above, we believe that the results of Beig et al.
 331 [2012] and Fadnavis and Beig [2006] (magenta triangles), agree very well with our estimates
 332 (red plusses) in both altitude ranges (both panels of Figure 3). Note in particular the rapid change
 333 from negative to positive values near 75-80 km. In Figure 3, the left panel at 4°N was chosen in
 334 part to compare further with Figure 4, and the right panel at 20°N was chosen to compare with
 335 Beig et al.,[2012] results based on composite data in the 0-30° latitude band. We note that our
 336 results show that there can be significant differences of responses at various latitudes.
 337



338
 339 **Figure 3.** Ozone responses to solar decadal cycle versus altitude, at 4°N, from 50 to 100 km (left panel), and 20°N,
 340 from 20 to 60km (right). Values are responses at solar max minus responses at solar min (% /100sfu). Magenta
 341 triangles denote results by Beig et al. [2012], average of responses at 6 and 18 hrs local time, and 0-30°N. Red
 342 plusses denote our estimate (average at 6 and 18 hrs). Green asterisks denote our estimate at 6hrs, and blue
 343 diamonds, estimate at 18hrs.
 344

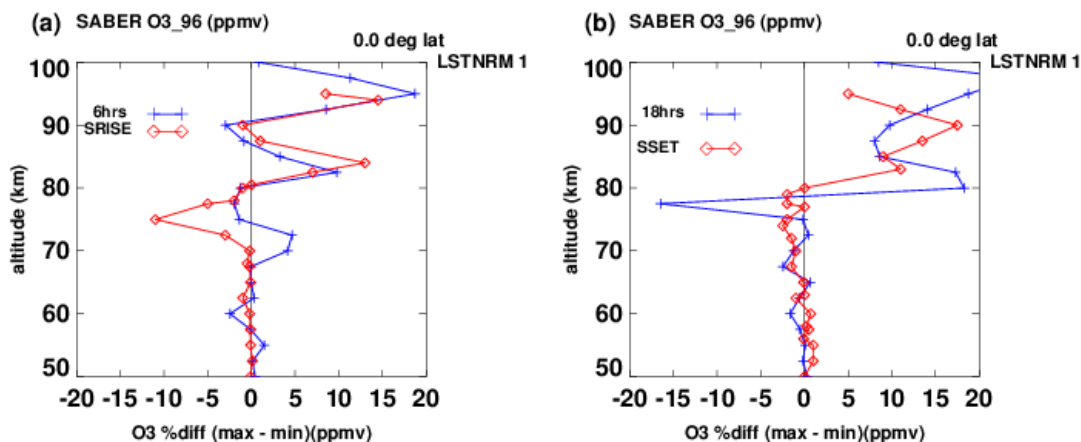
345 Figure 4 shows ozone responses to solar activity versus altitude, from 50 to 100 km, at the
 346 equator for sunrise (left) and sunset (right). Values are responses at solar max minus those at
 347 solar min (% /100sfu). Red diamonds denote responses found by Beig et al. [2012] at 6 hrs (left
 348 panel) and 18 hrs (right), composite from 0-4°N. Blue plusses denote our corresponding results
 349 based on SABER data.

350 It is the only instance where Beig et al.,[2012] show responses separately for 6 and 18hrs.

351 Except for the large negative values (red diamonds) from Beig et al [2012] in the left panel
 352 near 74 km, and the large negative value (blue plusses) by us at 77.5 km in the right panel, we
 353 believe that the comparisons are mostly favorable, in view of uncertainties discussed earlier.
 354 Although not shown, the half width of the error bars provided by Beig et al.,[2012] between 80
 355 to 90 km are $\sim \pm 10$ ((% /100sfu)

356 This can be compared with our results in the left panel of Figure 3 at 4°N. It is seen that
 357 although there are sharp variations above 70km, the agreements are at least qualitatively good,
 358 considering the caveats noted above.

359 The large excursions near 75 km are not isolated, but are systematic for both Beig et al.,
 360 [2012] and us, as can be seen further in Figure 6 for 16°N.



361 **Figure 4.** Ozone responses to solar activity versus altitude, from 50 to 100 km, at the equator. Values are responses
 362 at solar max minus responses at solar min (% /100sfu). Left panel: Red diamonds denote results based on HALOE
 363 data by Beig et al. [2012] at 6 hrs (left panel) and 18 hrs (right) local time, composite from 0-4°N. Blue plusses
 364 denote our results based on SABER data at 6hrs and 0 deg (left panel) and 18hrs (right).
 365
 366

367 3.2 Results: Temperature responses at 6, 18hrs (sunrise and sunset)

368 Figure 5 corresponds to Figure 3, but for temperature. Values are responses at solar max minus
 369 responses at solar min (°K /100sfu).

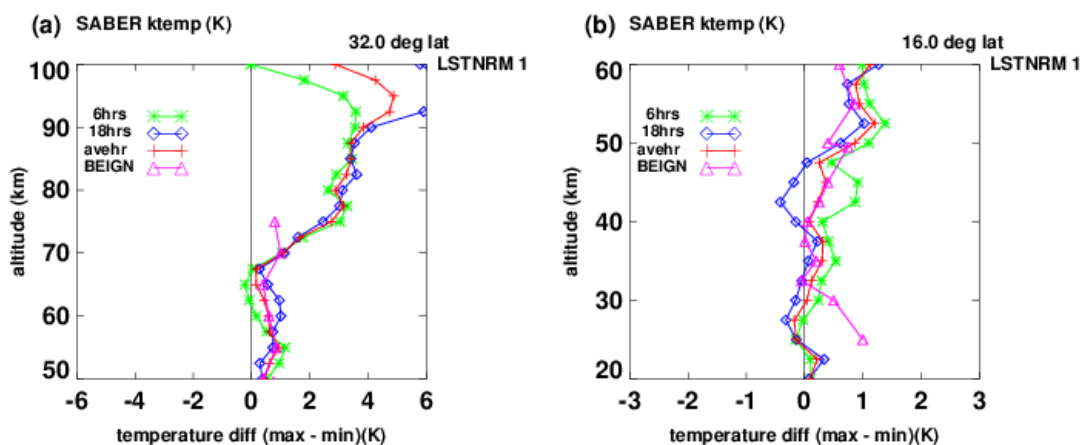
370 The left panel shows our and Beig et al.,[2012] temperature responses from 50 to 100 km, at
 371 32°N. The magenta triangles show responses based on HALOE data, by Beig et al. [2012] for
 372 temperature (composite, 0-30°N, BEIGN), which are averages of sunrise and sunset responses,
 373 and should be compared with the red plusses which denote the average of our results at 6hrs and
 374 18hrs. It can be seen that the agreement of our averages (magenta triangles and red plusses) are
 375 very favorable, except at 75km. Beig et al.,[2012] do not provide temperature responses above
 376 75 km. The green asterisks denote our results for 6hrs and the blue diamonds denote our
 377 responses at 18 hrs. Beig et al.,[2012] do not provide results separately for 6 and 18hrs.

378 The right panel corresponds to the left panel, but at 16°N and 20 to 60km, and the HALOE
 379 results are from Fadnavis and Beig [2006], 0-30°N composite. Above 30km, the agreements of
 380 our averages (magenta triangles and red plusses) are very favorable. We note that according to
 381 Fadnavis and Beig [2006] and Remsberg et al. [2002], that at altitudes below ~35km (~5hPa),
 382 HALOE uses temperatures from the National Center for Environmental Prediction (NCEP).

383 This could be the reason for the differences between the magenta triangles and our red plusses
 384 below 35 km.

385 It can be seen that even in the stratosphere, the responses at 6hr are different from those at
 386 18hrs. We note that the left panel represents results at 32°N, instead of 16°N, as the agreement
 387 with results by Beig et al. [2012] is somewhat better.

388
 389



390
 391
 392 **Figure 5.** Corresponds to Figure 3, but for temperature responses to solar activity versus altitude, from 50 to 100 km
 393 (left panel), and 20 to 60 km (right). Values are responses at solar max minus responses at solar min °K /100sfu.
 394 Magenta triangles denote results by Beig et al. [2012], averaged of 6 and 18 hrs local time (composite 0-30°N). Red
 395 plusses denote our estimate (average of 6 and 18 hrs, at 32°N (left panel)) and 16°N, right panel), based on SABER
 396 data. Green asterisks denote our estimates at 6hrs, and blue diamonds are estimates at 18hrs.

397

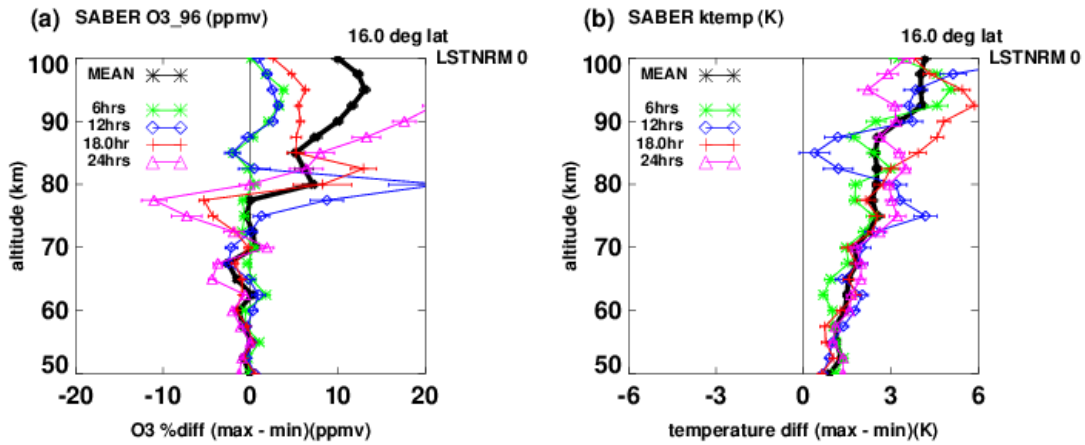
398 4.0 Ozone and temperature responses over a diurnal cycle.

399 In this section, we extend our results to other local times. Although the figures show responses
 400 only at 6, 12, 18, and 24 hrs, we have generated hourly responses, and can do so at any local
 401 time. We do not believe that plots at additional local times would add important information for
 402 purposes here, and would make other details less discernible.

403 Generally, previous studies based on other satellite measurements do not describe how they
 404 treat data with respect to local times, and we cannot make comparisons as with HALOE.
 405 Some studies use different data from various instruments, which mix data measured at different
 406 local times. See Section 5.2 and the discussion in reference to Figure 9, for details.

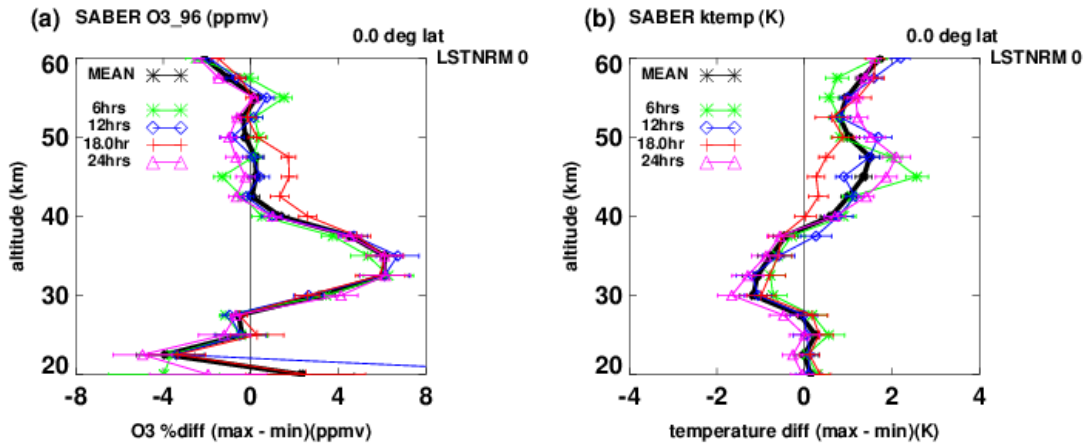
407 Figure 6 shows our ozone (left panel) and temperature (right panel) responses from 50 to 100
 408 km, at 16°N over a diurnal cycle (6, 12, 18, 24hrs). The black line denotes our responses based
 409 on SABER data where the zonal means are averages over both longitude and 24 hrs of local
 410 time. The green asterisks denote responses for 6hrs, blue diamonds (12hrs), red plusses (18hrs),
 411 and magenta triangles (24 hrs).

412 Up to this point, ozone values are responses at solar max minus responses at solar min
 413 (percent/100sfu). In the following, note that unlike the situation above at 6 and 18hrs for ozone at
 414 specific local times, the normalizing values used to obtain responses in percent are now averaged
 415 over local time, to be consistent with responses based on zonal means that are averages over both
 416 longitude and local time (black line in Figure 6).
 417
 418



419
 420 **Figure 6.** Ozone (left panel) and temperature (right) responses from 50 to 100 km at 16°N. Values are responses
 421 at solar max minus responses at solar min (% /100sfu) for ozone and °K/100sfu for temperature. Black asterisks
 422 denote responses based on zonal means that are averages over both longitude and local time. Green asterisks denote
 423 our responses based on zonal means fixed at 6hrs, blue diamonds fixed at 12hrs, red plusses at 18 hrs, and magenta
 424 triangles at 24hr, based on SABER data.
 425

426 Figure 7 shows the ozone (left panel) and temperature (right panel) responses to solar activity
 427 versus altitude, at the Equator, from 20 to 60 km, at 6hrs (green asterisks), 12hrs (blue
 428 diamonds), 18hrs (red plusses), 24 hrs (magenta triangles), and based on zonal means that are
 429 averages over local times (black asterisks). For ozone, below about 40 km, diurnal variations
 430 have relatively little effect on responses. For temperature, the effects can be larger, even at
 431 altitudes as low as 30 km.
 432
 433



434

435 **Figure 7.** As in Figure 6, but from 20 to 60 km. Ozone (left panel) and temperature (right) responses at 0°. Values are
436 responses at solar max minus responses at solar min (% /100sfu) for ozone and °K/100sfu for temperature. Black
437 asterisks denote our responses based on zonal means that are averages over both longitude and local time. Green
438 asterisks denote our responses of zonal means at 6hrs, blue diamonds at 12hrs, red plusses at 18 hrs, and magenta
439 triangles at 24hrs, based on SABER data.

440

441 Figures A1 and A2 of the Appendix present corresponding plots to Figure 7, but at 32° and 44°.

442

443 **5.0 Comparisons with responses based on operational satellite measurements (fixed or** 444 **drifting local times).**

445 In the stratosphere and lower mesosphere, previous global results of responses to the decadal
446 solar cycle have been largely based on data from the NOAA operational satellites (including the
447 Stratosphere Sounding Unit (SSU), the Microwave Sounding Unit (MSU), and the Solar
448 Backscatter Ultraviolet (SBUV) instruments). An advantage of the operational satellites is that
449 they can provide global measurements covering decades, being replaced as the instruments
450 degrade. However, issues of calibration, instrument offsets, stability, and continuity, can be
451 problematical. The satellites are generally polar orbiters and sun-synchronous, and make
452 measurements at two fixed local times, one for the satellite ascending mode, and one for the
453 descending mode.

454 As noted above, in merging data from different satellites, consistency in local times needs to
455 be considered. Tumman et al. [2015], in reviewing some of the data processing methods taken by
456 various groups, report that generally, diurnal variations are either neglected, or are assumed to be
457 negligible below ~ 45-50 km. See also Davis et al. (2015).

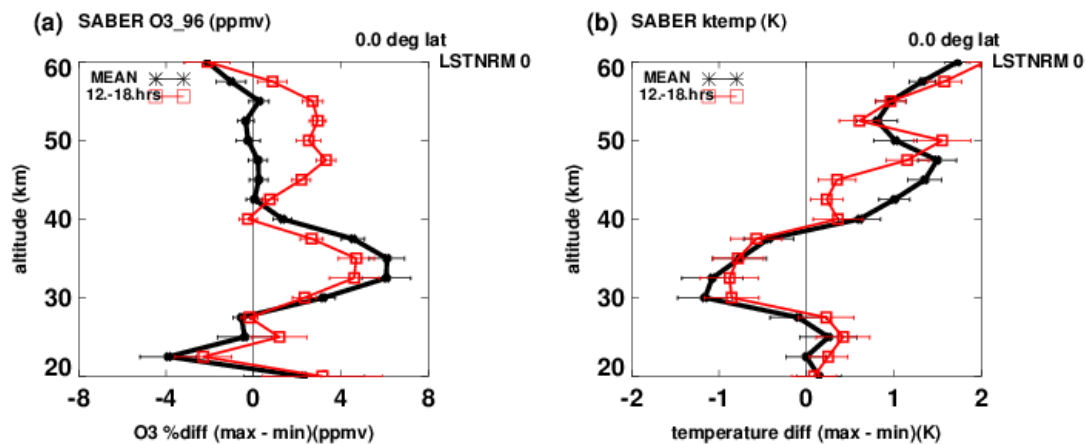
458

459 **5.1 Effects of local time variations due to satellite orbital drift**

460 As noted earlier, over years, the orbits of some satellites have drifted, so that the local times at
461 which measurements are made have also drifted by several hours, as described by McPeters et
462 al.,[2013].

463 To study the effects of local time changes due to orbital drift, from our estimates of diurnal
464 variations, we can simulate their effects on responses to solar variability. As a simple example,
465 Figure 8 shows our results for ozone (left panel) and temperature (right panel) responses to solar
466 activity versus altitude, at the Equator, from 20 to 60 km. Values are responses at solar max
467 minus responses at solar min in percent/100 sfu for ozone, and K/100 sfu for temperature. The
468 red squares denote results where local times increased linearly from 12 to 18 hrs from 2002 to
469 2014, to simulate orbital drift. Black asterisks denote responses based on zonal means that are
470 averages over both longitude and local time. It can be seen that there are significant differences
471 between them, especially above 40 km. We have also run tests with the local time varying at
472 different hours and durations, and the differences can be smaller or more pronounced than that
473 shown in Figure 8.

474



475 **Figure 8.** Ozone (left panel) and temperature (right panel) responses to solar activity versus altitude, at the Equator,
 476 from 20 to 60 km. Values are responses at solar max minus responses at solar min in % per 100 sfu for ozone, and
 477 K/100 sfu for temperature. Black asterisks denote responses based on zonal means that are averages over both
 478 longitude and local time. Red squares denote corresponding results, but with local times increasing linearly from 12
 479 to 18 hrs from 2002 to 2014.
 480
 481

482 5.2 Comparisons with operational satellite data

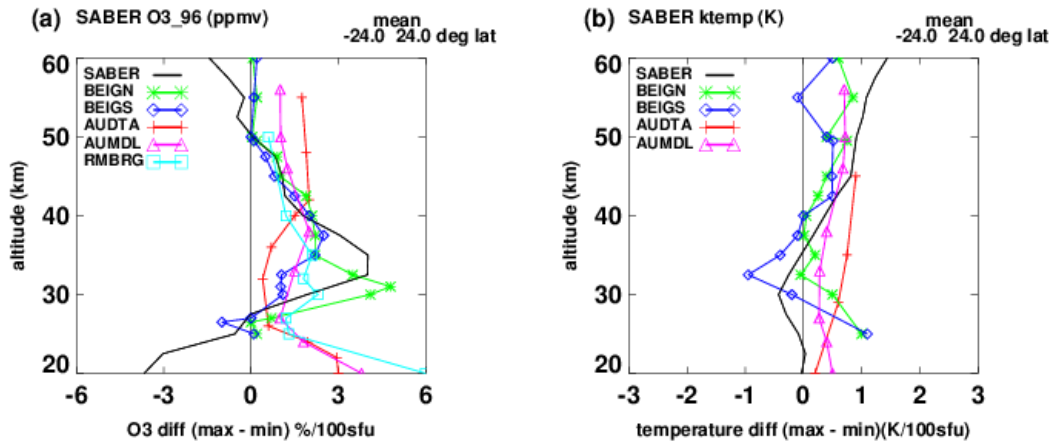
483 Unlike the above comparisons with results by Beig et al., [2012], based on HALOE data, other
 484 studies, such as those based on operational satellites, generally did not describe how they
 485 approached the issue of diurnal variations in detail. So we will not then attempt to make
 486 comparisons, but only present some previous findings. In addition to issues related to local times,
 487 there are been reports based on data-related issues in general. Details can be found in Austin et
 488 al., [2008], Crooks and Gray [2005], Gray et al. [2005], and Huang et al. [2016b].

489 Figure 9 is taken from our previous analysis (Huang et al. [2016b], Figure 3). It compares
 490 results from previous studies done by others, which were manually transferred by us, so they are
 491 not exact. Our ozone responses (black line, SABER) are shown in the left plot (a), versus altitude
 492 from 20 to 60 km, averaged from 24°S to 24°N, to better conform to results by others. The light
 493 blue squares represent results of Remsberg (2008, RMSBRG), the green asterisks are from
 494 Fadnavis and Beig (2006, BEIGN, 0-30°N), and the blue diamonds are from Beig et al., (2012,
 495 BEIGS, 0-30°S), all based on HALOE data.

496 The red line (plusses) in Figure 9(a) show ozone responses from Soukharev and Hood [2006]
 497 (AUDTA, data from 1979-2003), as reported by Austin et al. [2008], and from models (AUMDL,
 498 magenta lines and triangles), also reported by Austin et al. [2008], representing composite results
 499 from 25°S to 25°N latitude. The Soukharev and Hood [2006] results (red plusses) are a
 500 composite based on SBUV, HALOE, and SAGE data, that show a minimum near 30 km, and a
 501 maximum above 40 km.

502 The right plot in Figure 9(b) corresponds to the left plot, but for temperature. The temperature
 503 responses (AUDTA, data from 1979-1997) were taken by Austin et al. [2008] from Scaife et al.
 504 [2000]. In Figure 9(b), the black line denotes our responses based on SABER data, averaged
 505 from 24°S to 24°N, to conform to previous results by others.

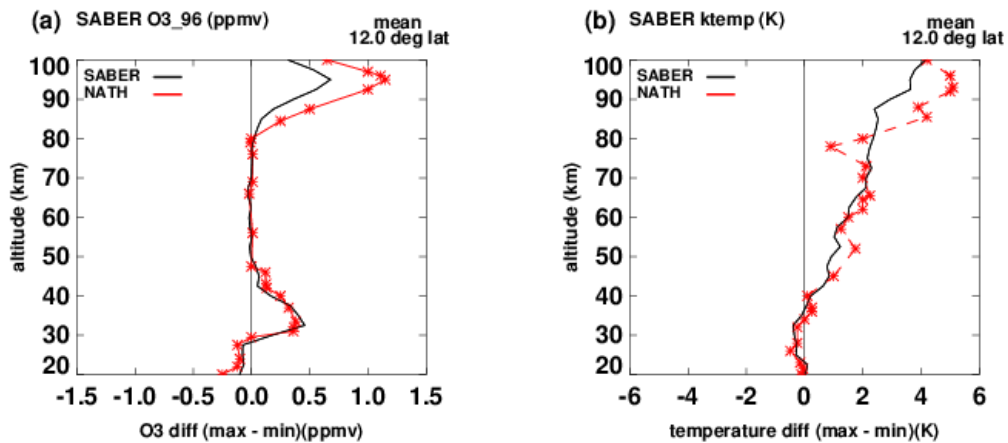
506 The issue of local time effects is not discussed in detail in these studies. As noted above,
 507 Austin et al., [2008] note that zonal means of models are averages over local time in contrast to
 508 those based on satellite measurements, which are typically at fixed local times.



509
 510 **Figure 9.** Left panel (a): ozone responses versus altitude from 20 to 60 km; black line: SABER results averaged
 511 from 24°S to 24°N; light blue squares: Remsberg (2008, RMSBRG); green asterisks: Fadnavis and Beig, [2006],
 512 BEIGN, 0-30°N; blue diamonds :BEIGS, 0-30°S, HALOE data; red plusses: Austin et al. [2008] data AUDTA;
 513 magenta triangles, Austin et al., [2008] model, AUMDL, 25°S to 25°N latitude composite. Right panel (b):
 514 temperature responses corresponding to left panel.

515
 516 Nath and Sridharan [2014] have also analyzed the same SABER data as we did and derived
 517 responses at 10–15° latitude. Plots comparing with our results are given in Figure 10 (taken from
 518 Figure 5 of Huang et al. [2016a]). Black lines denote our results and red asterisks denote that by
 519 Nath and Sridharan [2014]. For both ozone and temperature, their responses agree better with
 520 ours up to ~45km, but not so well at higher altitudes. We believe that the differences of the
 521 responses at higher altitudes are due to the local time variations in the SABER data, as discussed
 522 in Section 2. Nath and Sridharan (2014) do not appear to have considered diurnal variations.
 523 Note that in Figure 10 the ozone responses are not in percent differences, as in other plots, so that
 524 differences between 45 and 80 km are not readily discernible, due to their small values.

525
 526



527
 528 **Figure 10.** Ozone (left) and temperature (right) responses to solar activity vs. altitude, from 20 to 100 km. Values
 529 are responses at solar max minus responses at solar min in ppmv /100 sfu for ozone and K/100 sfu for temperature.

530 Black lines denote SABER responses at 12° lat; red color denotes results of Nath and Sridharan (2014), for 10–15°
531 lat, also based on SABER data.

532

533 **6.0 Data length and aliasing**

534 In Section 2.2.2, we noted that in the application of Equation (1), possible aliasing among the
535 different terms are not definitively addressed. In addition, it has been argued that more than one
536 solar cycle of data is more advantages. Following our analysis given in Huang et al.,[2016b], we
537 address these issues in this section.

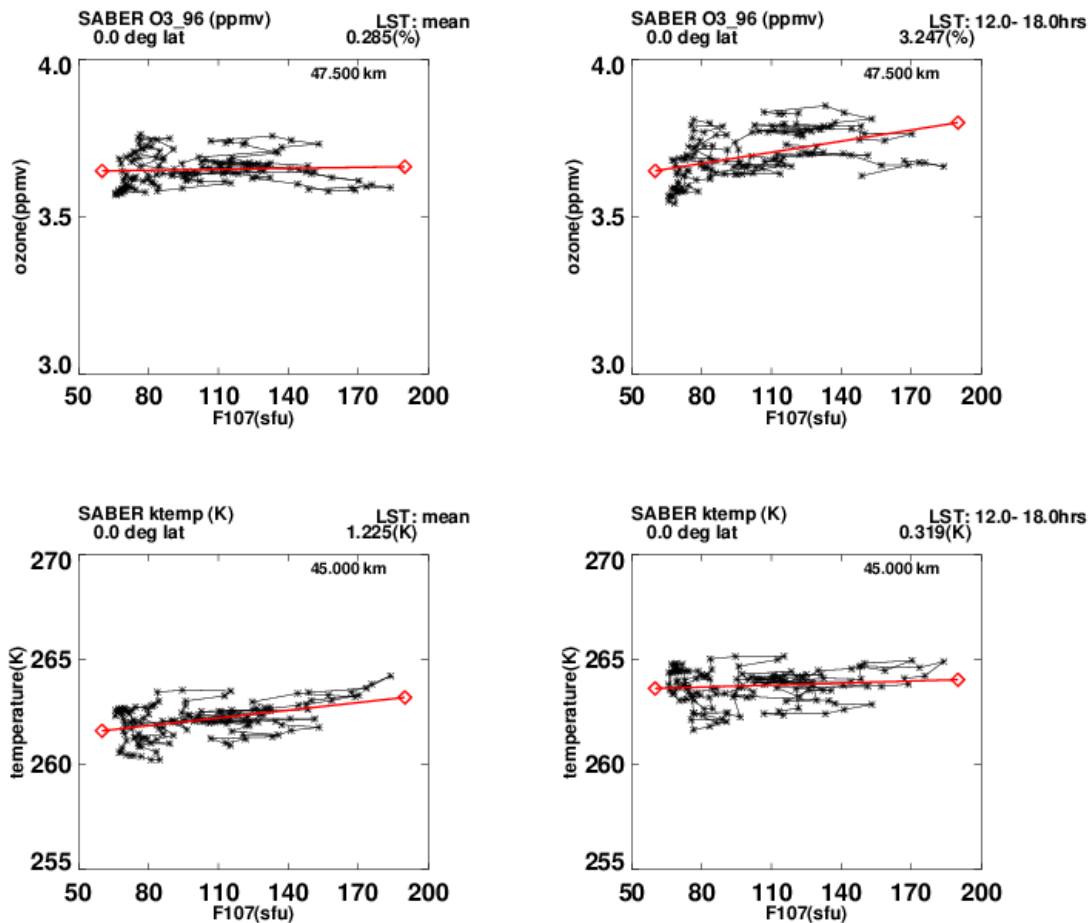
538 Figure 11 is a scatter diagram plot of monthly values versus the 10.7 cm flux. The top row
539 shows ozone at 47.5 km at the Equator, the bottom row shows temperature at 45 km and the
540 Equator. The left panels represent the monthly zonal means that are averaged over both longitude
541 and local time, and the right panels use zonal means where the local times simulate orbital drift
542 as discussed in reference to Figure 8. The red lines in Figure 11 represent linear fits between the
543 monthly values and the 10.7 cm flux, which corresponds to using only the solar term (F107) of
544 the multiple regression (Eq. 1). For ozone (top row), the values 0.28 percent/100sfu (left header
545 label, left panel) and 3.24 percent/100sfu at 47.5 km (right panel) compare well with the
546 regression results which uses all terms of Eq. (1), seen in Figure 8 (left panel). For temperature
547 (bottom row), the values 1.23K/100sfu and 0.32K/100sfu at 45 km also compare well with the
548 right panel of Figure 8. Consequently, aliasing from other terms in Equation (1) is not
549 significant.

550 As for issues of data length, unlike time series data, where time increases monotonically with
551 data length, the 10.7 cm flux values remain within a fixed interval between solar minimum and
552 solar maximum (~70 and 200 sfu). In Fig. 11, the values span about one solar cycle. But even
553 over more solar cycles, the 10.7 cm flux values would only repeat and backfill in with values in
554 the same general area in Figure 11, effectively providing a more average result but not
555 necessarily reducing the uncertainty much otherwise.

556 It can be argued that even with more than one solar cycle of data available, analysis over
557 individual cycles should be made to analyze differences among solar cycles.

558

559



560
 561 **Figure 11.** Top row: scatter plot of ozone monthly values versus 10.7 cm flux (sfu) at 47.5 km and the Equator.
 562 Left: monthly values are zonal means, including average over local time. Right: as in left panel, but zonal means
 563 include simulated local time variations of orbital drift. Bottom row: as in upper row, but for temperature monthly
 564 values. Red lines: linear fit between monthly values and 10.7 cm flux. Compare with Figure 8.
 565

566 7.0 Summary and discussion.

567 Using SABER data, we have investigated the effects of ozone and temperature diurnal
 568 variations on their responses to the solar cycle, from 2002 to 2014, and 20 to 100 km.

569 We find that for ozone, above ~ 40km, zonal means reflecting specific local times (e.g., 6, 12,
 570 18, 24 hrs) lead to different values of responses compared to each other, and compared to
 571 responses based on zonal means that are averaged over the 24 hours of local time (Figures 6,7).
 572 For temperature, effects of diurnal variations are not negligible at ~30 km and above.

573 We also have considered the variations of local times themselves due to orbital drifts of
 574 certain operational satellites, and their effects on responses to the solar cycle (Figure 8). The
 575 differences can be significant above ~35 km.

576 The quality and validity of our analysis are shown in comparisons with responses found by
 577 Beig et al., [2012], and Fadnavis and Beig, [2006], based on HALOE data, which made
 578 measurements only at sunrise and sunset. Comparisons with our corresponding results, based on
 579 SABER measurements, are favorable, both at sunrise and sunset separately, and combined. Our
 580 analysis is robust in that the average of responses at specific local times over a diurnal period of

581 24 hrs is the same as responses based on zonal means that are averages over longitude and local
582 time together.

583 Previous studies based on other satellite data generally do not describe their treatment, if any,
584 of local times, so we cannot compare as for HALOE. Some studies also analyzed data merged
585 from different sources, with measurements made at different local times. As discussed in Section
586 5.2 in reference to Figure 9, the results of these studies do not generally agree very well among
587 themselves.

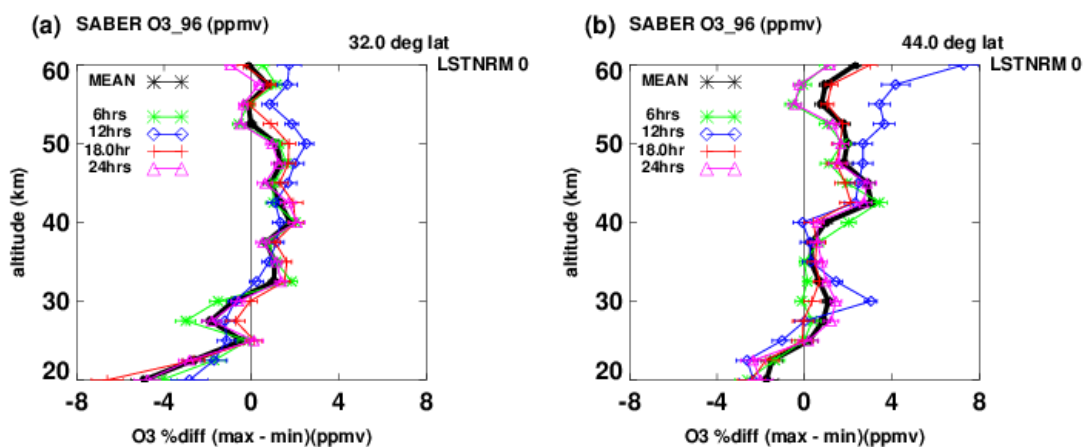
588 We do not believe that diurnal variations are the major reason for the discrepancies, as there
589 are likely other data-related issues. Other reasons for differences may be the conditions and
590 constraints under which the various measurements were made. Details can be found in Austin et
591 al., [2008], Crooks and Gray [2005], Gray et al. [2005], and Huang et al. [2016b].

592 However, diurnal variations should be included as part of the analysis of the differences
593 among various results.

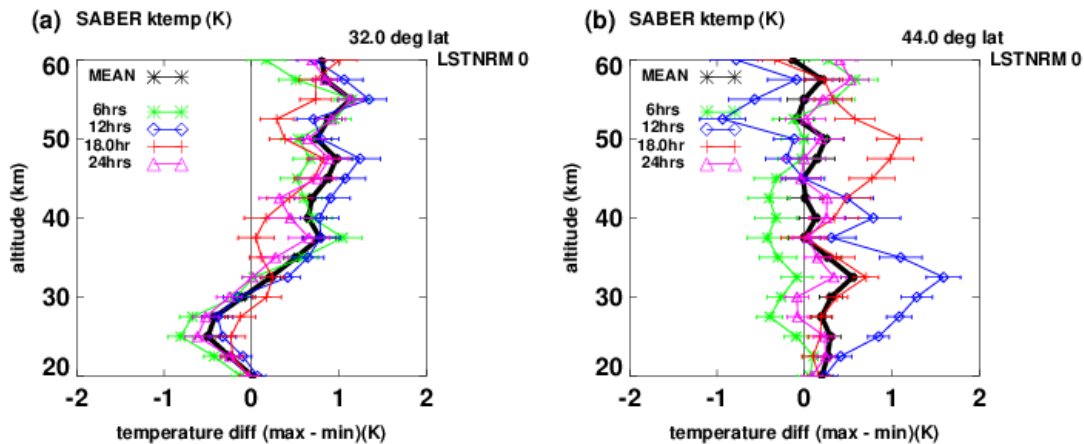
594 The effects due to satellite orbital drift (discussion in reference to Figure 8) may explain some
595 unexpected variations in the responses, especially above 40 km.

596
597
598
599
600

Appendix



601
602 **Figure A1.** As in Figure 7, Ozone responses at 32° (left panel) and 44° from 20 to 60 km. Values are responses at solar
603 max minus responses at solar min (% /100sfu) . Black asterisks denote our responses based on zonal means that are
604 averages over both longitude and local time. Green asterisks denote our responses of zonal means at 6hrs, blue
605 diamonds at 12hrs, red plusses at 18 hrs, and magenta triangles at 24hrs, based on SABER data.
606



607
 608
 609 **Figure A2.** As in Figure A1, but for temperature responses at 32° (left panel) and 44°, from 20 to 60 km. Values are
 610 responses at solar max minus responses at solar min ($^{\circ}\text{K}/100\text{sfu}$). Black asterisks denote our responses based on
 611 zonal means that are averages over both longitude and local time. Green asterisks denote our responses of zonal
 612 means at 6hrs, blue diamonds at 12hrs, red plusses at 18 hrs, and magenta triangles at 24hrs, based on SABER data.

613
 614

615 **Data availability**

616 The SABER data are freely available from the SABER project at <http://saber.gats-inc.com/>.

617

618 **Acknowledgements.** We thank editors P. Pisoft, C. Jacobi, and two anonymous reviewers,
 619 whose comments helped improve the manuscript.

620

621

622 **References**

623 Austin, J., Tourpali, K., Rozanov, E., Akiyoshi, H., Bekki, S., Bodeker, G., Bruhl, C.,
 624 Butchart, N., Chipperfield, M., Deushi, M., Fomichev, V. I., Giorgetta, M.A., Gray, L., Kodera,
 625 K., Lott, F., Manzini, E., Marsh, D., Matthes, K., Nagashima, T., Shibata, K., Stolarski, R. S.,
 626 Struthers, H., and Tian, W.: Coupled chemistry climate model simulations of the solar cycle in
 627 ozone and temperature, *J. Geophys. Res.*, 113, D11306, doi:10.1029/2007JD009391, 2008

628 Beig, G., Fadnavis, S., Schmidt, H., and Brasseur, G. P.: Inter-comparison of 11-year solar
 629 cycle response in mesospheric ozone and temperature obtained by HALOE satellite data and
 630 HAMMONIA model, *J. Geophys Res.*, 117, D00P10, doi:10.1029/2011JD015697, 2012

631 Bevington, P. R. and Robinson, D. K.: Data reduction and error analysis for the physical
 632 sciences, McGraw-Hill, New York, USA, 1992.

633 Brasseur, G. P.: The response of the middle atmosphere to long term and short-term solar
 634 variability: A two-dimensional model, *J. Geophys. Res.*, 98, 23,079–23,090,
 635 doi:10.1029/93JD02406, 1993.

636 Brasseur, G. P. and Solomon, S.: *Aeronomy of the Middle Atmosphere*, Springer, Dordrecht,
 637 the Netherlands, 2005.

638 Chapman, S., and R. S. Lindzen (1970), *Atmospheric Tides*, Springer, New York.

639 Crooks, S. A. and Gray, L. J.: Characterization of the 11-year solar signal using multiple
 640 regression analysis of the ERA-40 dataset, *J. Clim.*, 18, 996–1015, 2005.

641 Davis, S. M., Karen H. Rosenlof, Birgit Hassler, Dale F. Hurst, William G. Read, Holger
642 Vöme, Henry Selkirk, Masatomo Fujiwara, and Robert Damadeo, The Stratospheric Water and
643 Ozone Satellite Homogenized (SWOOSH) database: a long-term database for climate studies,
644 Earth Syst. Sci. Data, 8,461-490, 2016.

645 Fadnavis, S., and Beig, G: Decadal solar effects on temperature and ozone in the tropical
646 stratosphere, Ann. Geophys., 24, 2091–2103, 2006.

647 Frith, S. M., Kramarova, N. A., Stolarski, R. S., McPeters, R. D., Bhartia, P. K., and Labow, G.
648 J.: Recent changes in column ozone based on the SBUV version 8.6 merged ozone dataset, J.
649 Geophys. Res.-Atmos., 119, 9735–9751, doi:10.1002/2014JD021889, 2014.

650 Gille, S. T., A. Hauchecorne, and M.-L. Chanin (1991), Semidiurnal and
651 diurnal tidal effects in the middle atmosphere as seen by Rayleigh lidar,
652 J. Geophys. Res., 96, 7579–7587.

653 Gray, L. J., Haigh, J. D., Harrison, R. G.: A Review of The Influence of Solar Changes on the
654 Earth's Climate, Hadley Centre technical note 62, 1-81, 2005

655 Haigh, J.D., Austin, J., Butchart, N., Chanin, M-L., Crooks, S., Gray, L. J., Halenka, T.,
656 Hampson, J., Hood, L. L., Isaksen, ISA, Keckhut, P., Labitzke, K., Langematz, U., Matthes, K.,
657 Palmer, M., Rognerud, B., Tourpali, K., and Zerefos, C.: Solar variability and climate: selected
658 results from the SOLICE project. *SPARC Newsletter No. 23*, 2004.

659 Hood, L. L., 2004: Effects of solar UV variability on the stratosphere. *Solar Variability and Its*
660 *Effects on Climate, Geophys. Monogr.*, Vol. 141, Amer. Geophys. Union, 2004

661 Hood, L. L. , Misios, S., Mitchell, D. M., Rozanov, E., Gray, L. J., Tourpali, K., Matthes, K.,
662 Schmidt, H., Chiodo, G., Thiéblemont, R., Shindell, D., Krivolutsky, A., Solar Signals in CMIP-
663 5 Simulations: The Ozone Response, Quarterly Journal Royal Meteorological Soc., 141, 2670-
664 2689, doi:10.1002/qj.2553, October, 2015

665 Huang, F. T., Mayr, H. G., Reber, C. A., Russell III, J. M., Mlynczak, M. G.: and Mengel, J.
666 G.: Ozone quasi-biennial oscillations (QBO), semiannual oscillations (SAO), and correlations
667 with temperature in the mesosphere, lower thermosphere, and stratosphere, based on
668 measurements from SABER on TIMED and MLS on UARS, J. Geophys. Res., 113, A01316,
669 doi:10.1029/2007JA012634, 2008a.

670 Huang, F. T., Mayr, H. G., Russell III, J.M., Mlynczak, M. G.: and Reber: C. A.: Ozone
671 diurnal variations and mean profiles in the mesosphere, lower thermosphere, and stratosphere,
672 based on measurements from SABER on TIMED, J. Geophys. Res., 113, A04307, doi:10.1029/
673 2007JA012739, 2008b.

674 Huang, F. T., McPeters, R. D., Bhartia, P. K., Mayr, H. G., Frith, S. M., Russell III, J. M., and
675 Mlynczak, M. G.: Temperature diurnal variations (migrating tides) in the stratosphere and lower
676 mesosphere based on measurements from SABER on TIMED, J. Geophys. Res., 115, D16121,
677 doi:10.1029/2009JD013698, 2010a.

678 Huang, F. T., Mayr, H. G., Russell III, J. M., and Mlynczak, M. G.: Ozone diurnal variations
679 in the stratosphere and lower mesosphere, based on measurements from SABER on TIMED,
680 J. Geophys. Res., 115, D24308, doi:10.1029/2010JD014484, 2010b.

681 Huang, F. T., Mayr, H. G., Russell III, J. M., and Mlynczak, M. G.: Ozone and temperature
682 decadal trends in the stratosphere, mesosphere and lower thermosphere, based on measurements
683 from SABER on TIMED, Ann. Geophys., 32, 935–949, 2014.

684 Huang, F. T., Mayr, H. G., Russell III, J. M., and Mlynczak, M. G.: Ozone and temperature
685 decadal responses to solar variability in the mesosphere and lower thermosphere, based on

686 measurements from SABER on TIMED, *Ann. Geophys.*, 34,29-40, doi:10.5194/angeo-34-129-
687 2016a.

688 Huang, F. T., H. G. Mayr, J. M. Russell III, and M. G. Mlynczak, Ozone and temperature
689 decadal responses to solar variability in the stratosphere and lower mesosphere, based on
690 measurements from SABER on TIMED, *Ann. Geophys.*, 34, 801–813, doi:10.5194/angeo-34-
691 801-2016, 2016b.

692 Keckhut, P., Cagnazzo, C., Chanin, M.-L., Claud, C., Hauchecorne, A.: The 11-year solar-
693 cycle effects on the temperature in the upper-stratosphere and mesosphere: Part I—Assessment
694 of observations, *Journal of Atmospheric and Solar-Terrestrial Physics* 67, 940-947, 2005.

695 McPeters, R. D., Bhartia, P. K., Haffner, D., Labow, G. J., and Flynn, L.: The version 8.6
696 SBUV ozone data record: An overview, *J. Geophys. Res.-Atmos.*, 118, 8032–8039,
697 doi:10.1002/jgrd.50597, 2013.

698 Nath, O., and Sridharan, S.: Long-term variabilities and tendencies in zonal mean TIMED–SABER
699 ozone and temperature in the middle atmosphere at 10–15°N, *J. Atmos. Solar-Terr. Phy.*, 120, 1–8,
700 2014.

701 Maycock, A., K. Matthes, S. Tegtmeier, R. Thiéblemont, and L. Hood, The representation of
702 solar cycle signals in stratospheric ozone – Part 1: A comparison of satellite observations,
703 *Atmos. Chem. Phys.*, doi:10.5194/acp-2015-882, 2016

704 Mitchell, D. M., L.J.Gray, M. Fujiwara, T. Hibino, J. A. Anstey, W. Ebisuzaki, Y. Harada, C.
705 Long, S. Misios, P. A. Stott, and D. Tan, Signatures of naturally induced variability in the
706 atmosphere using multiple reanalysis datasets, *Q. J. R. Meteorol. Soc.*, 141, 2011-2031,
707 doi:10.1002/qj.2492, 2014.

708 Mukhtarov, P., Pancheva, D., and Andonov, B.: Global structure and seasonal and interannual
709 variability of the migrating diurnal tide seen in the SABER/TIMED temperatures between 20
710 and 120 km, *J. Geophys. Res.*, 114, A02309, doi:10.1029/2008JA013759, 2009.

711 Oberheide, J., M. E. Hagan, W. E. Ward, M. Riese, and D. Offermann (2000), Modeling the
712 diurnal tide for the Cryogenic Infrared Spectrometers and Telescopes for the Atmosphere
713 (CRISTA) 1 time period, *J. Geophys. Res.*, 105, 24,917–24,929.

714 Randel, W. J., Shine, K. P., Austin, J., Barnett, J., Claud, C., Gillett, N. P., Keckhut, P.,
715 Langematz, U., Lin, R., Long, C., Mears, C., Miller, A., Nash, J., Seidel, D. J., Thompson, D. W.
716 J., Wu, F., and Yoden, S., An update of observed stratospheric temperature trends, *J. Geophys.*,
717 114, doi:10.1029/2008JD010421, 2009. Remsberg, E. E., Bhat, P. P., and Deaver, L. E.:
718 Seasonal and long-term variations in middle atmosphere temperature from HALOE on UARS, *J.*
719 *Geophys. Res.*, 107, D19, 4411,
720 doi:10.1029/2001JD001366, 2002.

721 Remsberg, E. E.: On the response of Halogen Occultation Experiment (HALOE) stratospheric
722 ozone and temperature to the 11-year solar cycle forcing *J. Geophys. Res.*, 113, D22304,
723 doi:10.1029/2008JD010189, 2008

724 *J. Geophys. Res.*, 90, 5733–5743, 1985.

725 Russell, III J. M., Mlynczak, M. G., Gordley, L. L., Tansock, J., and Esplin, R.: An overview
726 of the SABER experiment and preliminary calibration results, *Proceedings of the SPIE*, 44th
727 Annual Meeting, Denver, Colorado, July 18-23, 3756, 277–288, 1999.

728 Sakazaki, T., M. Fujiwara, C. Mitsuda, K. Imai, N. Manago, Y. Naito, T. Nakamura, H.
729 Akiyoshi, D. Kinnison, T. Sano, M. Suzuki, and M. Shiotani, Diurnal ozone variations in the
730 stratosphere revealed in observations from the Superconducting Submillimeter-Wave
731 Limb-Emission Sounder (SMILES) on board the International

732 Space Station (ISS), *J. Geophys. Res.: Atmospheres*, 118, 2991–3006, doi:10.1002/jgrd.50220,
733 2013.

734 Sakazaki, T., Shiotani, M., Suzuki, M., Kinnison, D., Zawodny, J. M., McHugh, M., and
735 Walker, K. A.: Sunset–sunrise difference in solar occultation ozone measurements (SAGE II,
736 HALOE, and ACE-FTS) and its relationship to tidal vertical winds, *Atmos.*
737 *Chem. Phys.*, 15, 829–843, doi:10.5194/acp-15-829-2015, 2015.

738 Shindell D, Rind, D., Balachandran, J., Lean, J., and Lonergran, P.: Solar cycle
739 variability, ozone and climate. *Science*, 284, 305-308, 1999.

740 Scaife, A. A., J. Austin, N. Butchart, M. Keil, S. Pawson, J. Nash, and I. N.
741 James (2000), Seasonal and interannual variability of the stratosphere diagnosed from UKMO
742 TOVS analyses, *Q.J.R. Meteorol. Soc.*, 126, 2585–2604.

743 Soukharev, B. E., and L. L. Hood (2006), The solar cycle variation of stratospheric ozone:
744 Multiple regression analysis of long-term satellite data sets and comparisons with models, *J.*
745 *Geophys. Res.*, 111, D20314, doi:10.1029/2006JD007107.

746 Tummon, F., B. Hassler, N. R. P. Harris, J. Staehelin, W. Steinbrecht, J. Anderson, G. E.
747 Bodeker, A. Bourassa, S. M. Davis, D. Degenstein, S. M. Frith, L. Froidevaux, E. Kyrölä, M.
748 Laine, C. Long, A. A. Penckwitt, C. E. Sioris, K. H. Rosenlof, C. Roth, H.-J. Wang, and J. Wild,
749 Intercomparison of vertically resolved merged satellite ozone data sets: interannual variability
750 and long-term trends, *Atmos. Chem. Phys.*, 15, 3021-3043, 2015

751 Zeng, Z., W. Randel, S. Sokolovskiy, C. Deser, Y.-H. Kuo, M. Hagan, J. Du, and W. Ward
752 (2008), Detection of migrating diurnal tide in the tropical upper troposphere and lower
753 stratosphere using the Challenging Minisatellite Payload radio occultation data, *J. Geophys. Res.*,
754 113, D03102, doi:10.1029/2007JD008725.

755 Zhang, X., Forbes, J. M., Hagan, M. E., Russell III, J. M., Palo, S. E., Mertens, C. J., and
756 Mlynchzak, M. G.: Monthly tidal temperatures 20–120 km from TIMED/SABER, *J. Geophys.*
757 *Res.*, 111, A10S08, doi:10.1029/2005JA011504, 2006.

758